Chemistry and Physics of Lipids 169 (2013) 95–105

Contents lists available at SciVerse ScienceDirect

Chemistry and Physics of Lipids

journal homepage: www.elsevier.com/locate/chemphyslip

Free energy of WALP23 dimer association in DMPC, DPPC, and DOPC bilayers

Norberto Castillo[a], Luca Monticelli[b,c,d], Jonathan Barnoud[b,c,d], D. Peter Tieleman[a,*]

[a] Department of Biological Sciences and Institute for Biocomplexity and Informatics, University of Calgary, 2500 University Drive N.W., Calgary, Alberta T2N 1N4, Canada
[b] INSERM, UMR-S665, DSIMB, Paris F-75015, France
[c] Universitè Paris Diderot, Sorbonne Paris Citè, UMR-S665, Paris F-75013, France
[d] INTS, Paris F-75015, France

ARTICLE INFO

Article history:
Received 26 November 2012
Received in revised form 30 January 2013
Accepted 1 February 2013
Available online 13 February 2013

Keywords:
Helix–helix interaction
Molecular simulation
Hydrophobic mismatch
Helix dimerization
Lipid perturbation
Lipid–protein interactions

ABSTRACT

The MARTINI coarse-grained model is used to gain insight into the association of WALP23 helices in three different lipid membranes: DMPC, DPPC and DOPC. Potentials of mean force describing the association of two WALP23 helices embedded in different lipid bilayers indicate no barrier of association and a stabilization of more than 20 kJ mol^{-1} of the associated state relative to the fully dissociated state. Association is strongest in DMPC, followed by DPPC and DOPC. Helix–helix association appears to be enthalpically favorable in all lipid bilayers, while the entropic contribution appears favorable only in the presence of significant positive hydrophobic mismatch, in DMPC lipids. The interpretation of this requires care given the coarse-grained nature of the simulations, but the sign of the thermodynamic quantities agrees with experimental measurements on dimerization of $(AALALAA)_3$ peptides and the observed association free energies are within the experimental range. Both protein–protein and lipid–lipid interactions appear to strongly favor protein dimerization, while the interactions between a dimer and lipid are unfavorable relative to the interactions between two separated monomers and lipids. Dimers with antiparallel orientation appear to be thermodynamically favored over parallel dimers, particularly in conditions of greater hydrophobic mismatch, but elucidating the detailed origin of this likely requires simulations of helices for which there is structural data on the dimer. We analyze 3D density, membrane order, and membrane thickness maps using new freely available analysis programs. Although these properties differ somewhat for each lipid, perturbations extend to about 1 nm for lipid density, ~2 nm for ordering and ~2.5 nm for thickness. A striking feature is the appearance and extent of systematic density fluctuations around the helices.

1. Introduction

Cellular membranes consist of a phospholipid bilayer and a variety of proteins that are involved in a wide range of essential physiological processes. Membrane proteins are the primary connection between the inside and the outside of cells, for example acting as cell surface receptors (He and Hristova, 2012), as transporters of nutrients, metabolites (Giacomini et al., 2010) and other molecules including entire proteins (Driessen and Nouwen, 2008), as conduits for a variety of signals (Rosenbaum et al., 2009), and as key player in cellular processes such as endocytosis (Doherty and McMahon, 2009) and fusion (Sudhof and Rothman, 2009). In many cases, these processes involve changes in structure of transmembrane domains, including domain motions, dimerization of transmembrane helices, and larger-scale conformational changes. Therefore, understanding the relationships between sequence, structure, dynamics and functions of membrane proteins is of wide interest in many fields of medicine, biology, biochemistry, and physical chemistry.Functional proteins can be formed in the membrane via the association of domains with well-defined structure – for instance, in helical proteins, the association of previously inserted transmembrane helices. This is a key event in membrane protein folding and assembly (MacCallum and Tieleman, 2011; White and von Heijne, 2004; Wimley, 2012; Woolhead et al., 2004). Significant effort has been devoted to understand the driving forces and thermodynamics of this process in detail (Cymer et al., 2012; Fink et al., 2012; Langosch and Arkin, 2009; MacKenzie and Fleming, 2008; Strandberg et al., 2012). The association of proteins in membranes depends both on specific protein–protein interactions and on less specific protein–lipid interactions. For instance, it is well known that the transmembrane GxxxG motif of Glycophorin A (GpA) contributes to the formation of a stable right-handed helix dimer in membranes (Fleming and Engelman, 2001) – a clear example of specific protein–protein interaction, although this motif only occurs in a relatively small number of proteins and does not explain the binding affinity of a larger set of GpA mutants, thus encouraging

* Corresponding author. Tel.: +1 403 220 2966.
E-mail address: tieleman@ucalgary.ca (D.P. Tieleman).

0009-3084
http://dx.doi.org/10.1016/j.chemphyslip.2013.02.001

the search for a broader explanation of helix–helix aggregation (Li et al., 2012). Protein association also depends on protein–lipid interactions. For example, a recent simulation study by Janosi et al. highlighted the importance of hydrophobic mismatch (i.e., the difference between protein hydrophobic length and the thickness of the hydrophobic region in the membrane, defined as positive when the protein hydrophobic length is longer than the hydrophobic thickness of the membrane) in determining the stability of GpA dimers in lipid membranes (Janosi et al., 2010a,b). In addition to direct protein–protein and protein–lipid interactions it is also quite plausible that indirect interactions such as lipid-mediated helix–helix interactions play an important role. Experimental studies have confirmed the key role played by membrane thickness on the association process of membrane proteins (Orzaez et al., 2005).

Specific and aspecific contributions are difficult to distinguish when studying biologically relevant proteins. Model systems are therefore a useful tool both in experiments and computational studies. Computational models range in complexity from two-dimensional idealized cylinders (Lague et al., 2001) and simplified particle-based simulations (Benjamini and Smit, 2012; de Meyer et al., 2008) to detailed atomistic models of proteins (Psachoulia et al., 2010). The use of small membrane proteins and model peptides with tunable features for experimental studies has been a particularly powerful approach that many research groups have followed to elucidate basic principles of transmembrane helix interactions (Killian and Nyholm, 2006; Langosch and Arkin, 2009; Vostrikov et al., 2010).

WALP23 (GWW(LA)$_8$LWWA) is one such model peptide that has been widely used as a model for more complex membrane proteins. WALP23 was designed in part to minimize protein–protein interaction to probe the effects of helix-bilayer hydrophobic mismatch on peptide behavior (de Planque and Killian, 2003; de Planque et al., 1998, 2001). Yet, fluorescence spectroscopy experiments showed a weak attractive peptide–peptide interaction between WALP23 helices (Sparr et al., 2005a). For these reasons, WALP23 appears to be an ideal system to study generic aspects of protein association in membranes.

Ash et al. carried out detailed free energy calculations on WALP23 and polyleucine, with excellent agreement in thermodynamic properties between coarse-grained MARTINI simulations and experimental measurements (Ash, 2009). Schafer et al. (2011) recently reported a computer simulation study combined with optical microscopy on WALP peptides (WALP23 and WALP31) in lipid membrane mixtures, proving that peptide association depends on the hydrophobic mismatch and determines partitioning of WALP between liquid crystalline and gel phases. Kim and Im (2010) performed molecular dynamics simulations on single WALP helices of different lengths (WALP16, WALP19, WALP23, and WALP27) in different lipid membranes. Even though the aim of this study was not directly related to the association event of WALP helices and the time scale was shorter than is likely required for full sampling (Monticelli et al., 2010; Schafer et al., 2011; Sengupta and Marrink, 2010), it did provide significant insight into helix-bilayer hydrophobic mismatch effects. Free energy profiles using as reaction coordinate the tilt angle of the helix with respect to the normal axis of the membrane suggested that the tilting of the helix is the major response to a hydrophobic mismatch. Similar qualitative results have been also observed in KALP peptides (GKK(LA)$_n$LKKA)(de Planque et al., 2001; Kandasamy and Larson, 2006; Killian and Nyholm, 2006). We also note that PMF calculations with MARTINI have recently been published for the interaction between two rhodopsins, a 7-helix G-protein coupled receptor (Periole et al., 2012).

WALP23 has been also used as a model peptide to determine helix orientation in the association process. Pyrene fluorescence experiments have shown that association between WALP23 peptides under conditions of hydrophobic mismatch primarily occurs when the helices are oriented antiparallel with respect to each other (Monticelli et al., 2010; Sparr et al., 2005b). Dithionite quenching experiments on Ac-(LALAAAA)$_3$-amide and fluorescence resonance energy transfer experiments on NBD-(AALALAA)$_3$-NH$_2$ yielded similar conclusions (Yano et al., 2002, 2006, 2011).

In this manuscript we present a detailed study of the antiparallel and parallel association of WALP23 helices in three different lipid membranes (DPPC, DMPC, and DOPC) at the coarse-grained level using the MARTINI force field (Marrink et al., 2007; Monticelli et al., 2008). We calculate potentials of mean force as a function of the lateral separation between the peptides in three different lipid membranes: DMPC, DPPC and DOPC, with different hydrophobic thicknesses and area per lipid. We are interested in features of the potential of mean force and membrane structure, in particular at a distance where one might imagine a single lipid between the two helices. In the association profile of two hydrophobic helices in aqueous solution there is a clear barrier in the enthalpy component when water no longer fits between the two helices, but this is compensated by an entropic well because water is no longer trapped in between helices (MacCallum et al., 2007). Similarly, in lipid bilayers a single lipid in between two helices might cause an entropic barrier, but it is also possible that lipids are too flexible to be an important factor. We analyze the lipid structure at different points along the PMF and make an attempt to elucidate the microscopic driving forces for helix aggregation, including the role of hydrophobic mismatch, helix orientation, and lipid properties.

2. Methods

2.1. System set up

The coarse-grained structures of antiparallel and parallel WALP23 dimers were generated using a four-to-one mapping from previous atomistic structures obtained by Sparr et al. (2005a). The minimum distance between the centers of mass of both helices was fixed at 0.75 nm by aligning the axes of both helices with the bilayer normal and translating one helix along the *X* axis. Additional structures were created with a larger separation (see below). The structures were then embedded in pre-equilibrated coarse-grained lipid bilayers (DMPC, DPPC, and DOPC) followed by a water solvation step using a procedure described by (Kandt et al., 2007). A typical snapshot is shown in Fig. 1. In MARTINI, DMPC has three tail beads per acyl chain, DPPC four tail beads per acyl chain, and DOPC five tail beads per chain, with the middle slightly less apolar (MARTINI type C3 instead of C1) and the angle between that bead and the two beads adjacent to it is 120° instead of 180° in saturated hydrocarbon chains. The three bilayers consisted of 272 lipids (136 per leaflet) and the total number of water molecules was 4872.

2.2. Molecular dynamics simulations and potential of mean force calculations

All molecular dynamics (MD) simulations were carried out using the GROMACS 4.0.5 software package (Hess et al., 2008) and the MARTINI force field (Marrink et al., 2007; Monticelli et al., 2008). Non-bonded interactions were calculated within a cutoff of 1.2 nm using shift functions (shift between 0.9 and 1.2 nm for Lennard–Jones interactions, between 0 and 1.2 nm for electrostatics). These parameters are standard for the MARTINI force field. Prior to potential of mean force calculations, energy minimization of the system was carried out with the steepest descent algorithm. For each system, minimization was followed by a short equilibration run (2.5 ns). The temperature of the systems was set to 325 K

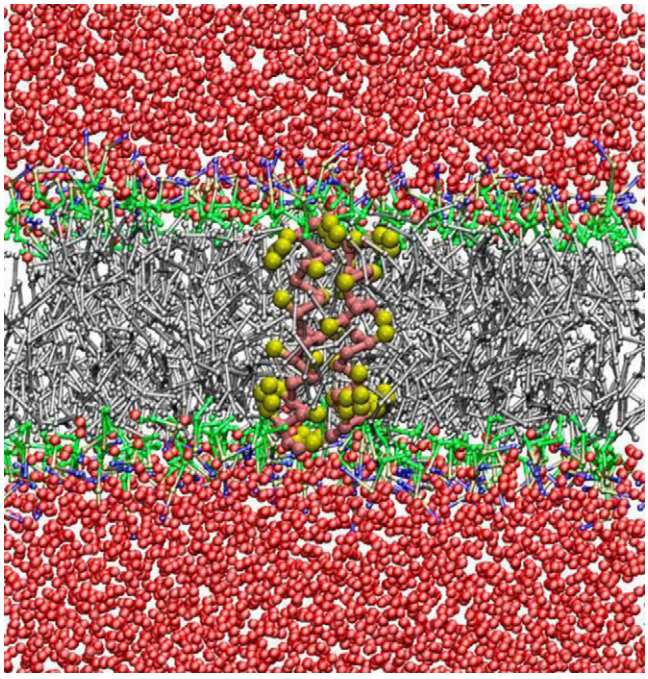

Fig. 1. Snapshot for the simulation system where the centers of mass of WALP23 helices are separated by 0.75 nm. Balls and sticks are used to identify the components of the system. WALP23 helices are shown in yellow and pink, lipid head group atoms are shown in blue, tan and green, lipid tails are shown in gray, and water molecules are shown in red. (For interpretation of the references to color in this figure legend, the reader is referred to the web version of this article.)

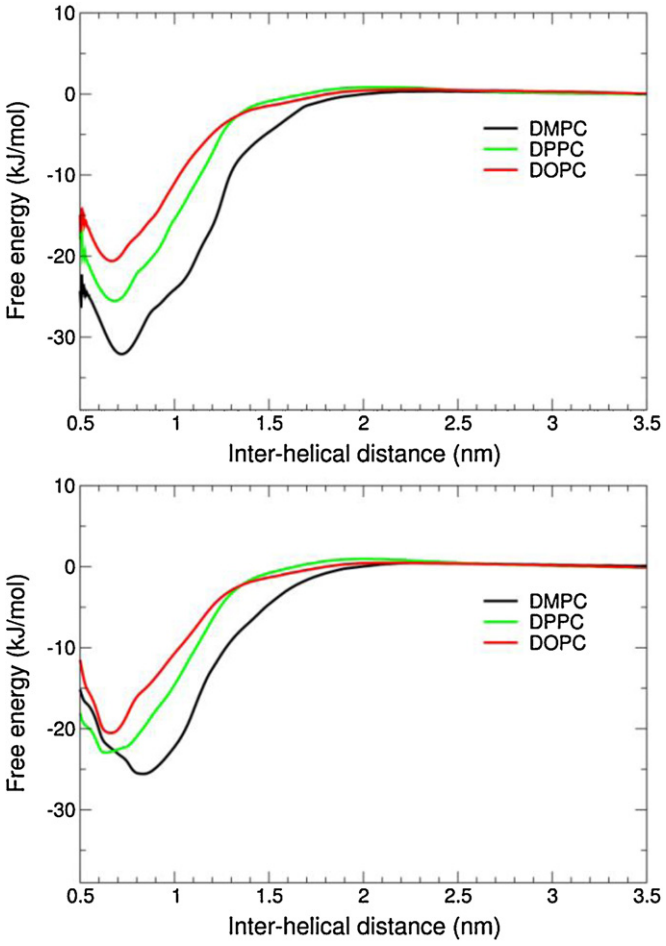

Fig. 2. Antiparallel (top) and parallel (bottom) association PMFs of WALP23 helices in DMPC (black), DPPC (green), and DOPC (red). The distance reported is the distance between the centers of mass of the two peptides. (For interpretation of the references to color in this figure legend, the reader is referred to the web version of this article.)

using the Berendsen weak coupling method (Berendsen et al., 1984) with a coupling time of 0.1 ps. The pressure was set to 1 bar using a semi-isotropic coupling scheme with lateral and perpendicular pressures coupled separately with coupling time 0.1 ps and compressibility of 2×10^{-5} bar^{-1} (Berendsen et al., 1984). We used an integration time step of 25 fs in all simulations. The same conditions were used during equilibration and during the umbrella sampling runs.

The umbrella sampling algorithm (Torrie and Valleau, 1977) was used to carry out the potential of mean force (PMF) calculations. The umbrella sampling windows were generated using the pull code of GROMACS with a force constant of 2200 kJ mol^{-1} nm^{-2}, starting from the initial structure where the inter-helical distance was 0.75 nm (Fig. 1). A total of 28 windows (structures) with spacing of 0.1 nm were created spanning the range of inter-helical distance 0.75–3.45 nm. Each window was equilibrated for 2 μs before a production simulation of 16 μs. Nine additional windows at separations of 0.65, 0.70, 0.725, 0.775, 0.80, 0.825, 0.875, 0.90, 0.925 nm with a force constant of 3000 kJ mol^{-1} nm^{-2} were created to improve sampling at the inter-helical distance where formation of the associated state takes place. The weighted histogram analysis method (Kumar et al., 1992; Roux, 1995) (WHAM) was used to unbias the umbrella window potentials. With the degree of sampling in the simulations used, the statistical uncertainty in potentials of mean force and structural properties is minimal, as can be judged from the smooth profiles based on independent adjacent windows in most analyses. In addition, we

Table 1
Summary of simulations performed in this work, along with structural features of the membrane systems. For the bilayer thickness and peptide length, the average values are reported with the standard error in parentheses.

System	Lipid	Number of lipids	Simulation length (μs)[a]	Bilayer hydrophobic thickness (nm)[b]	Peptide hydrophobic length (nm)[b]
Monomer	DOPC	256	5	2.92 (0.01)	2.67 (0.01)
	DPPC	256	5	2.63 (0.01)	2.63 (0.01)
	DLPC	256	5	1.94 (0.01)	2.58 (0.02)
Parallel orientation	DOPC	272	16 × 32	2.91 (0.01)	2.66 (0.01)
	DPPC	272	16 × 32	2.63 (0.01)	2.64 (0.01)
	DLPC	272	16 × 32	1.94 (0.01)	2.62 (0.02)
Antiparallel orientation	DOPC	272	16 × 32	2.91 (0.01)	2.67 (0.01)
	DPPC	272	16 × 32	2.63 (0.01)	2.64 (0.01)
	DLPC	272	16 × 32	1.94 (0.01)	2.61 (0.01)

[a] Production only; equilibration time was 2 μs for each simulation.
[b] Calculated in the simulations at contact distance.

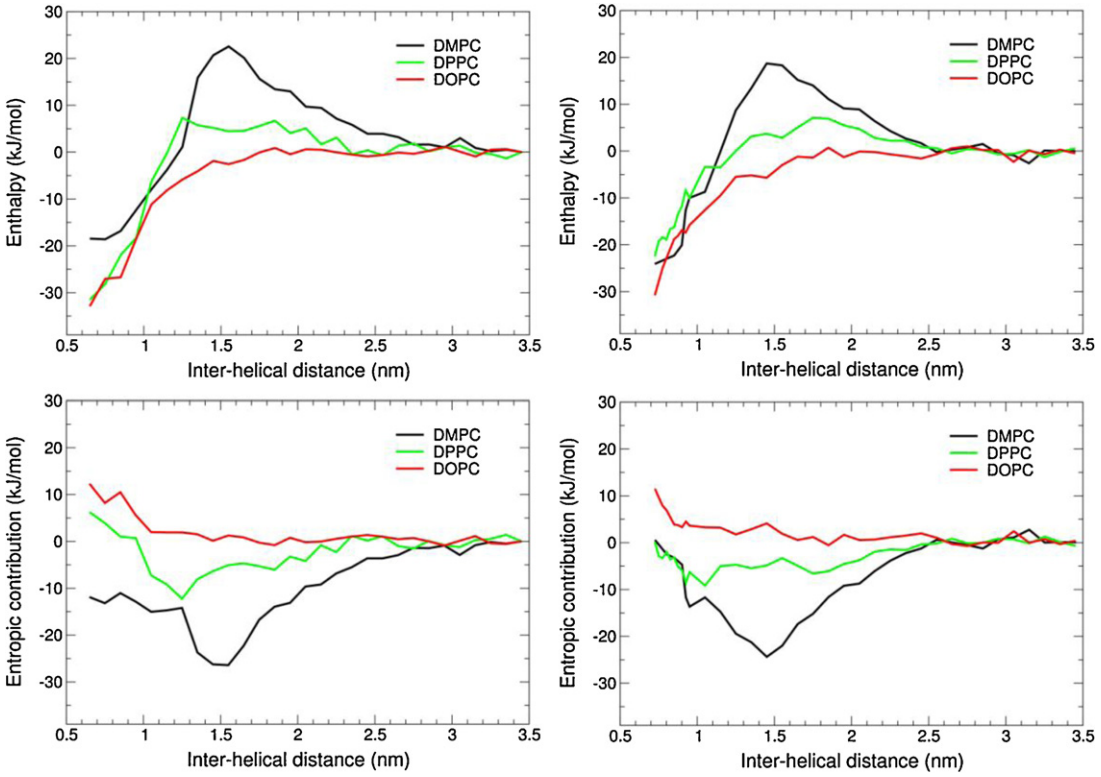

Fig. 3. Potential energy (top) and entropy $-T\Delta S$ (bottom) profiles for the antiparallel and parallel association of WALP23 helices in DMPC (black), DPPC (green), and DOPC (red). The graphs are aligned at zero at maximum separation of the helices. (For interpretation of the references to color in this figure legend, the reader is referred to the web version of this article.)

calculated PMFs based on subsets of the simulation data, shown in Supplementary Fig. 1.

2.3. Membrane density, membrane thickness and lipid ordering

Partial density, membrane thickness and lipid ordering plots were calculated using new analysis software, available for download free of charge (http://www.dsimb.inserm.fr/~luca/downloads/). The metrics were calculated on a grid with spacing of about 0.2 nm, so each element of volume (voxel) was about 0.2 nm × 0.2 nm × Z nm, where Z is the dimension of the box in the direction of the membrane normal. Partial densities were calculated as the average mass of the particles present in the voxel divided by the volume of the voxel; only lipids and proteins were taken into account. The lipid order parameter, defined as $P = 1/2 < 3\cos^2\theta - 1 >$, where θ is the angle between the bond vector and the membrane normal, was calculated for all bonds in the lipid acyl chains and then averaged within each voxel over the ensemble of bonds and over time. Membrane thickness was calculated as the distance, in each voxel, between the average positions of the lipid phosphate group (PO4 bead) in the two leaflets calculated on 10 non-overlapping frames and averaged over time. All analyses of membrane perturbation required precise removal of the translational motion of the peptides (i.e., the position of the center of mass of both peptides was constant), obtained with standard GROMACS tools.

3. Results

3.1. Average hydrophobic thickness and mismatch

We estimated the hydrophobic thickness of the lipid bilayers as the average distance between the centers of mass of the first hydrophobic bead in the lipid tails in the two leaflets (Table 1). The calculation was performed for all umbrella windows of each particular system, and showed no significant difference among windows. The hydrophobic thickness of the bilayers follows the trend DOPC (2.91 nm) > DPPC (2.63 nm) > DMPC (1.94 nm). The length of the hydrophobic part of the peptide was calculated as the distance between the centers of mass of residues Leu4 and Leu20 (as in ref. Monticelli et al., 2010), and was approximately constant in all simulations, with values between 2.58 and 2.67 nm. We therefore find a small negative hydrophobic mismatch for DOPC systems, a small positive mismatch for DPPC and a significant positive mismatch for DMPC.

3.2. Thermodynamics of WALP23 association in lipid bilayers

Fig. 2 shows the PMFs obtained for the antiparallel and parallel helix association of WALP23 in the three different bilayers. In all cases the profiles show no free energy barrier for peptide dimerization, and a deep minimum corresponding to the associated state. The free energy of dimerization increases with decreasing membrane thickness (i.e., increasing hydrophobic mismatch). In all cases, the free energy profiles reach the plateau regime at inter-helical distances of ~2.25 nm. The minimum in the free energy profile is found at an inter-helical distance of ~0.7 nm for both types of association (parallel and antiparallel) in all three lipid bilayers, except for the parallel association in DMPC, where the minimum is at ~0.8 nm.

Taking advantage of extensive sampling, we can decompose the free energy profiles into enthalpy and entropy components. We obtain the free energy change ΔG from the potential of mean force, the enthalpy change ΔH directly from the total energy (ignoring the pressure-volume term which is negligible in the simulations), and ΔS from the relationship $\Delta G = \Delta H - T\Delta S$. Doing this, we ignore the

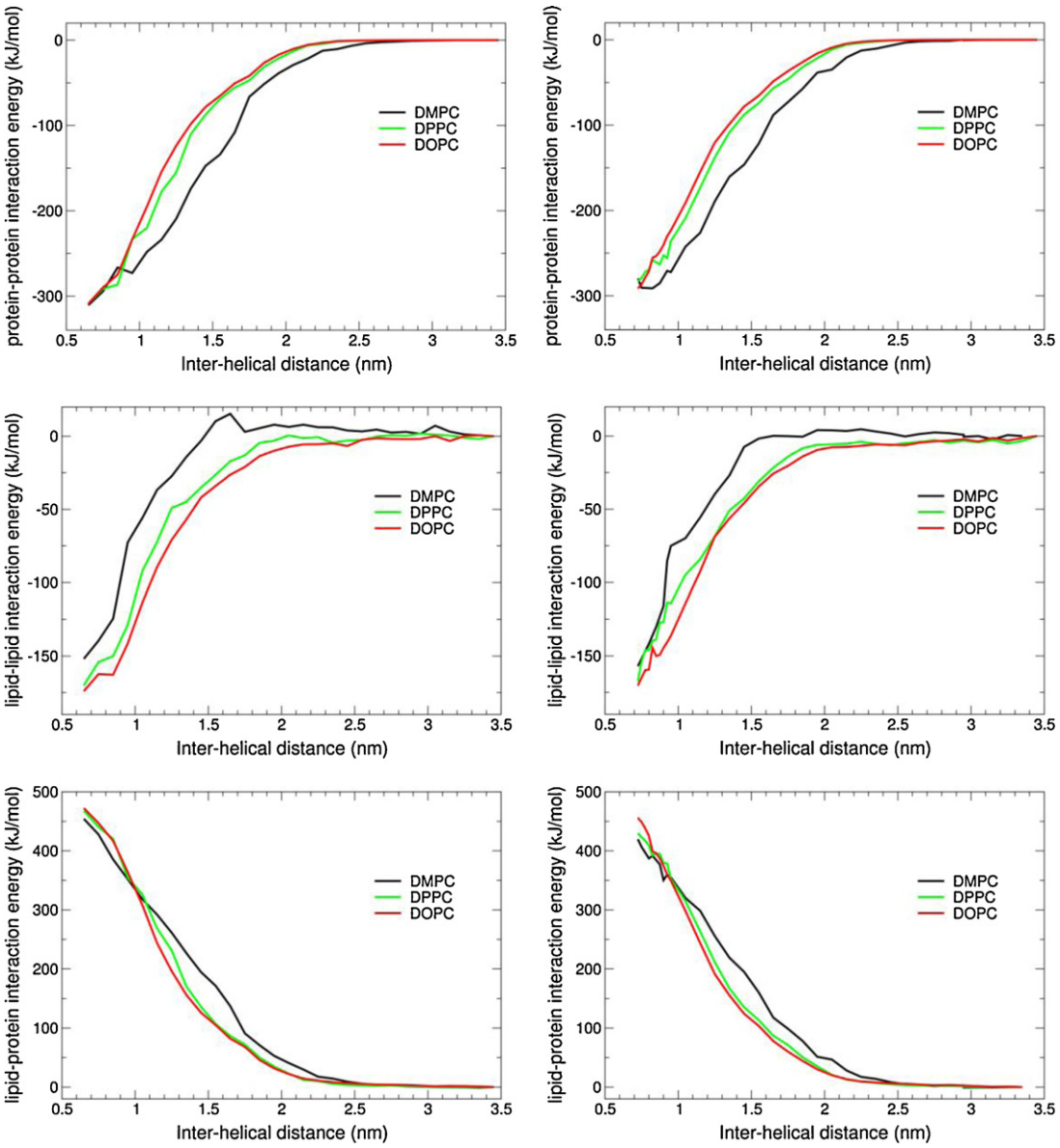

Fig. 4. Protein–protein (top), lipid–lipid (middle) and protein–lipid (bottom) interaction energy as a function of inter-helical separation distance, calculated for the antiparallel association of WALP23 helices in DMPC (black), DPPC (green), and DOPC (red). The energies are relative to the energies for the system with the largest helix–helix separation. (For interpretation of the references to color in this figure legend, the reader is referred to the web version of this article.)

possible effect of the umbrella potential, which modifies the total energy to a degree that can differ in each window. We also note that the interpretation of a breakdown of free energies into enthalpies and entropies requires significant caution in coarse-grained simulations, where large numbers of degrees of freedom are missing and in general the entropy-enthalpy balance that gives rise to a correct free energy is different from a more accurate atomistic simulation. This is obvious for the case of a PMF for two hydrophobic helices in MARTINI water, which shows the right free energy as function of distance but is almost entirely enthalpy driven, but a similar effect in the membrane cannot be excluded (Wu et al., 2011). On the other hand, previous PMF calculations give the right signs for enthalpy and entropy contributions (Ash, 2009), and the values we find here correspond approximately to experimental data (see below). Fig. 3 illustrates the potential energy profiles for the parallel and antiparallel association in DMPC, DPPC and DOPC.

We notice that, in all bilayers, WALP23 association appears to be enthalpically favorable, particularly in the case of lower hydrophobic mismatch. The entropic contribution appears to be favorable in the case of DMPC (large positive hydrophobic mismatch), although smaller than the enthalpic contribution. This may be due to a higher tilt angle in DMPC, perturbing more lipids than in the other two bilayers. In cases of small hydrophobic mismatch, the entropic contribution to the free energy profile is small and unfavorable at helix–helix contact distance.

While we observe no free energy barrier to protein dimerization, a potential energy barrier is present in all lipid bilayers. This barrier is significant in DMPC ($\sim$20 kJ mol^{-1} at $\sim$1.6 nm inter-helical distance), whereas it is less substantial in DPPC ($\sim$6 kJ mol^{-1}) and negligible in DOPC. At the same time, we observe no entropic barrier to helix association. In the case of DMPC, the entropic contribution is favorable and larger than the potential energy barrier, which results in the absence of a free energy barrier to helix association.

To gain better insight into the enthalpic component of the helix association process, we calculated the protein–protein, protein–lipid and lipid–lipid interaction energy as a function of

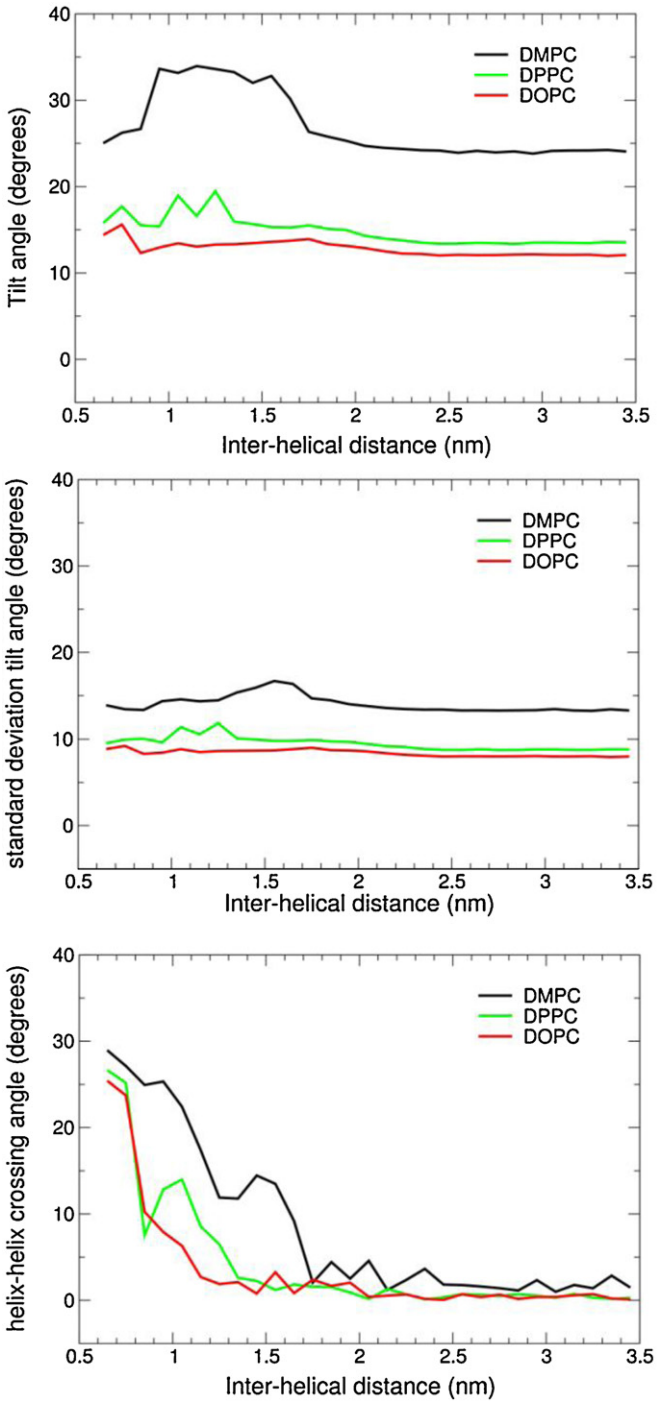

Fig. 5. Tilt angle (top), tilt angle standard deviation (middle), and helix–helix crossing angle (bottom) profiles of antiparallel association: Left panel (DMPC), middle panel (DPPC) and right panel (DOPC).

helix separation (Fig. 4). As expected, the associated state is highly stabilized by helix–helix interactions, whereas helix–lipid interactions are significantly unfavorable for the association event. The protein–protein interaction energy at the free energy minimum (~0.7 nm) appears to be largely independent of the lipid bilayer, suggesting similar packing of the helices. At larger distances (1.0–2.5 nm), helix–helix interaction energy profiles show some differences among the different bilayers, with the energy in DMPC being significantly lower (i.e., more favorable) than in the other bilayers.

As the peptides approach, protein–lipid interaction energy becomes less favorable. This can be explained by the decrease in the area of protein–lipid contact surface as the dimer is formed. It is interesting to notice that lipid–lipid interaction energy becomes more favorable as the proteins approach. In other words, we observe a favorable protein–protein interaction that is mediated by the lipids and has, at least in part, enthalpic origin. The lipid-mediated protein–protein interaction shows a clear dependence on the nature of the lipid: larger favorable contributions are observed with thicker lipid membranes.

A noticeable difference between antiparallel and parallel association is observed in DMPC, where $\Delta G_{\text{antiparallel}}$ is ~32.5 kJ mol^{-1} and $\Delta G_{\text{parallel}}$ is ~26 kJ mol^{-1}. The difference decreases with decreasing hydrophobic mismatch, and it disappears in the case of DOPC.

3.3. Interpreting thermodynamic data in terms of (microscopic) membrane structure

How does the thermodynamic view connect with the changes in the microscopic structure of the simulated systems? To answer this question, we explore how the membrane structure is affected by the presence of the peptides, and characterize how protein orientation and membrane perturbation change as the distance between the proteins is varied.

We noted above some significant differences in protein–protein interaction energy profiles in the different bilayers (Fig. 4). In particular, we noticed that the helix–helix interaction energy in DMPC is more favorable than in the other bilayers at separation distances between 1 and 2.5 nm. It appears likely that differences in protein–protein interaction energy are related to differences in helical orientation. We analyzed the orientation of the helices as a function of the structural properties of inter-helical distance (Fig. 5). The profiles of tilt angle and standard deviation of tilt angle in DMPC are significantly different from those in the other bilayers, particularly for the antiparallel orientation (see Fig. 5). Tilt angles in DMPC are about 7°–10° greater than in DPPC and DOPC for both the associated and dissociated states. This matches the results obtained by Kim and Im (2010) in their study of various WALP single helices in different lipid bilayers, as well as our previous results on WALP23 monomers and dimers.(Monticelli et al., 2010) The standard deviation of the helix tilt angle is also greater in DMPC, suggesting a higher mobility the helices.

The average crossing angle (the angle between the two helical axes) between helices is close to zero for the fully dissociated state in all three bilayers. The crossing angle increases as helices start to interact, reaching similar values at the contact distance (~29° in DMPC, ~26° in DPPC, and ~25° in DOPC). This suggests similar packing of the helices in the associated state, independent of the nature of the lipid bilayer. This is consistent with the values of the helix–helix interaction energy at contact, which are also very similar in all bilayers.

Lipid–lipid and lipid–protein interactions also play a role in determining the thermodynamics of helix association. Indeed, we notice differences in interaction energy profiles obtained in different lipid membranes (Fig. 4). How are these differences connected with membrane structure? We examined three metrics related to the membrane structure: lipid density, membrane thickness and lipid ordering.

Membrane thickness, lipid density and lipid ordering around transmembrane helical peptides are highly inhomogeneous, and they change as the distance between the proteins is varied. To better understand the effect of protein dimerization on lipid structure, we first examine the perturbation of membrane properties for isolated peptides (Fig. 6). In all membranes, lipid density seems to be relatively insensitive to the presence of the peptide. In DMPC lipids, membrane thickness and ordering are significantly higher in the

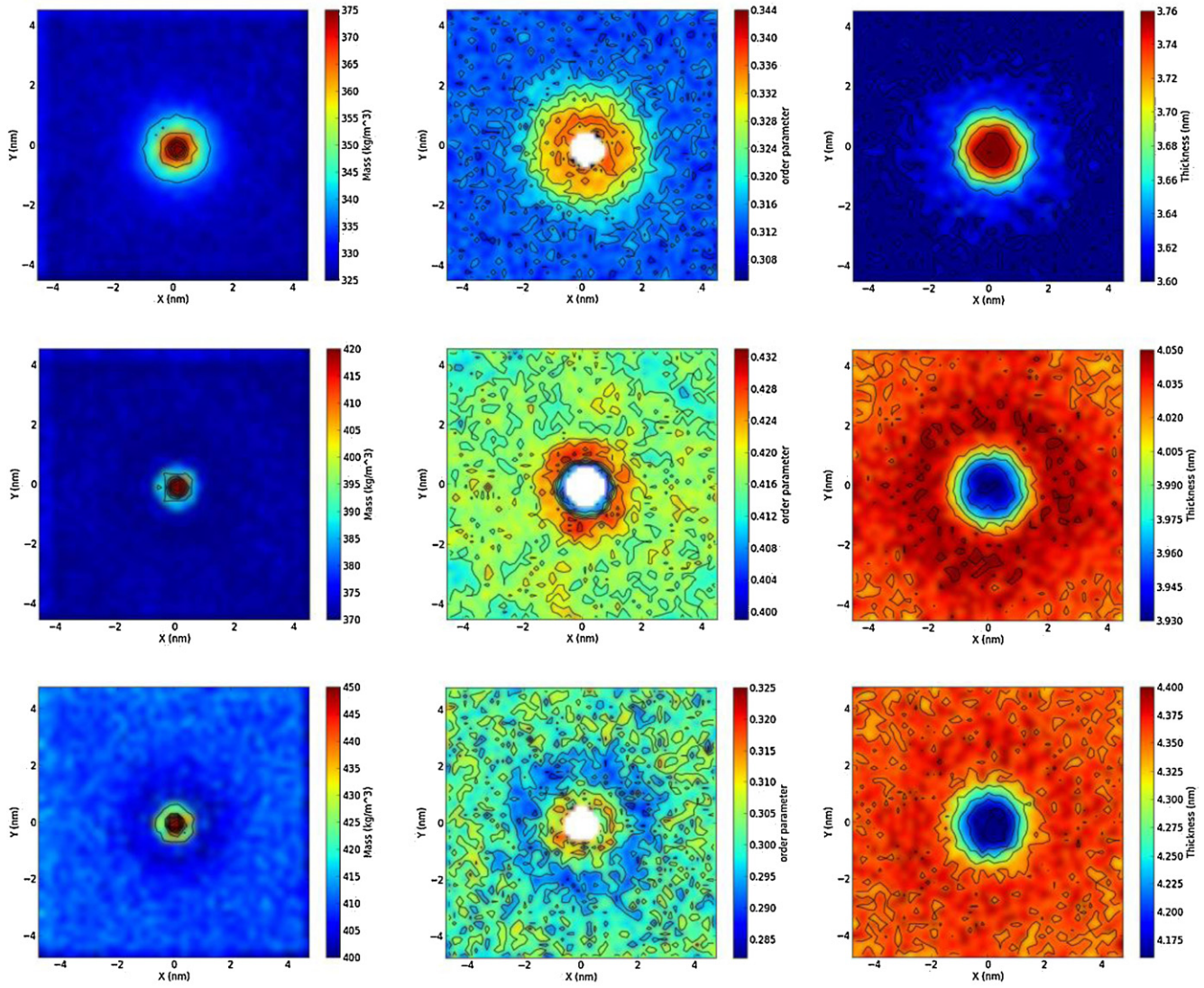

Fig. 6. Membrane partial density (left panels), lipid acyl chain order parameter (central panels), and membrane thickness (right panels) around a single WALP23 peptide in DMPC (top panels), DPPC (middle panels) and DOPC (bottom panels).

proximity of the peptide. This is consistent with the intuitive picture of the membrane stretching around the protein in conditions of positive hydrophobic mismatch. Membrane thickness is affected by the presence of the peptide to a much lesser extent in DPPC, but lipid ordering is again significantly higher for lipids in contact with the peptide. In DOPC, membrane thickness is significantly decreased in the proximity of the peptide, due to negative hydrophobic mismatch, and ordering changes in a non-monotonous fashion: lipid in the first solvation shell appear to be slightly more ordered than unperturbed lipids, but lipids in the second shell are less ordered than average unperturbed lipids.

The three metrics we used to characterize membrane structural perturbation are correlated, and they all can be used as markers of membrane perturbation, but they clearly provide different information. Lipid ordering appears to be more sensitive to the presence of protein inclusions. We also notice differences in the areas of the regions with perturbed membrane density, ordering and thickness. The perturbation extends to about 1 nm for lipid density, ~2 nm for ordering and ~2.5 nm for thickness.

We analyzed the perturbation of membrane structure also for simulations with WALP23 dimers. Fig. 7 shows membrane density, lipid ordering and membrane thickness for the case of parallel WALP23 peptides in DOPC at different distances. For all metrics, when peptides are at the maximum distance (3.45 nm), the two perturbed membrane regions still overlap although the PMFs have become effectively flat. Membrane density shows fluctuations in the region around the peptides. At large distances, the perturbation is similar to the effect of two isolated peptides, and the perturbation area has the shape of two sets of concentric rings (like a Fig. 8 shape). As the distance between the peptides gets shorter, the perturbed rings merge. At contact, the perturbed region has an ellipsoidal shape, with the peptides in the foci of the ellipse. While the patterns of the perturbation in density, ordering and thickness are qualitatively the same, differences in the extent of the perturbation are evident. Deviations in ordering and thickness are stronger than deviations in partial density of the lipids, and they involve larger portions of the membrane. As expected, for all metrics examined here the area of the perturbed region at contact is significantly less than the sum of the two perturbed areas observed for isolated peptides; hence the lipid–lipid interaction energy becomes more favorable as the peptides approach each other.

As expected, membrane perturbations are different in different lipids; the precise shape and extent of the perturbed areas strongly depend on the nature of the lipid but do not depend much on the

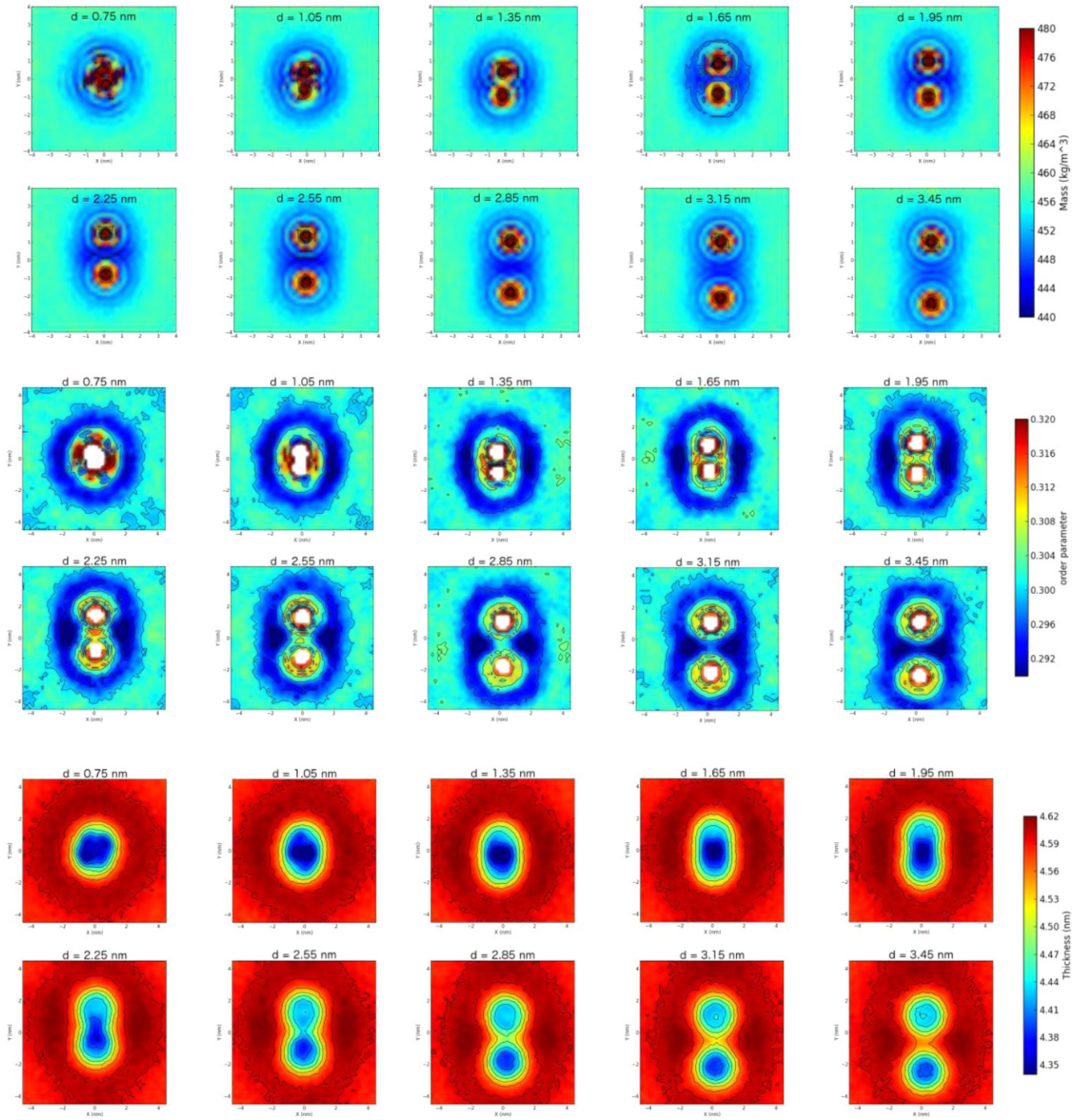

Fig. 7. Membrane partial density (top panels), lipid acyl chain order parameter (central panels) and membrane thickness (lower panels) as a function of the distance between centers of mass of the peptides, for WALP23 parallel association in DOPC.

orientation of the peptides (figure not shown). Yet, inspection of membrane perturbation for simulations in DMPC and DPPC leads to similar conclusions regarding the degree of perturbation (higher for thickness and ordering, lower for partial density) and the origin of lipid–lipid enthalpic gain upon aggregation.

Focusing on the lipid–lipid interaction energy profiles, the difference between DMPC and the thicker bilayers is greater at inter-helical distances of about 1.6 nm. At this particular distance the membrane thickness plots show considerably different distributions around the helices (Fig. 8): the perturbed region forms two concentric rings in the case of DMPC, while in DOPC the rings are completed fused into one distorted ring. Considering that the inter-helical distance is the same, the difference in lipid density distribution is likely due to a greater helical tilt in DMPC.

The difference in free energy between the parallel and antiparallel association is negligible in DOPC and it increases as positive hydrophobic mismatch increases, reaching the value of $\sim$6.5 kJ mol^{-1} in DMPC. Furthermore, the free energy minimum for the parallel orientation in DMPC is found at a distance of $\sim$0.8 nm, larger than in all other simulations ($\sim$0.7 nm). From the free energy breakdown it appears that the preference for the antiparallel orientation is due mostly to entropy: the entropic contribution is more

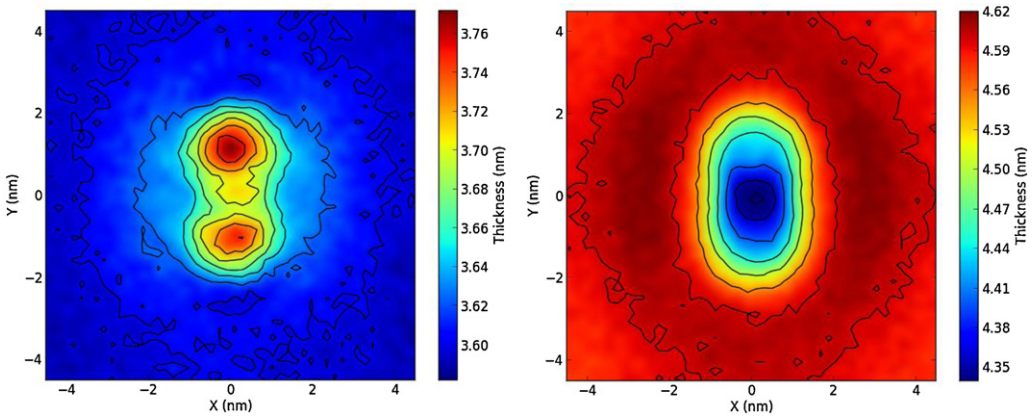

Fig. 8. Membrane thickness plots for parallel association at the inter-helical distance of 1.65 nm: DMPC (left panel) and DOPC (right panel).

favorable for the antiparallel dimer by almost 10 kJ mol^{-1}, while the enthalpy is less favorable by ~3.5 kJ mol^{-1} (see Fig. 3), despite both protein–protein and lipid–lipid interaction energies at contact being more favorable for the antiparallel case (see Fig. 9). As for the protein–protein interaction energy, the difference can be explained by different packing of the helices: the contact distance is lower in the antiparallel orientation (~0.7 nm instead of ~0.8 nm), while the helix–helix crossing angles at contact are very similar for both orientations. Bringing the helices at closer distance in the parallel orientation requires a sharp increase in the crossing angle (see Fig. 9), with a corresponding decrease in protein–protein interaction energy.

4. Discussion

Membrane protein association determines membrane protein topology, activity and aggregation. The association between helical protein segments depends both on specific and non-specific interactions. The latter are mediated by the lipids surrounding the protein, and are due to the perturbation of the membrane environment by the protein. Lipid-mediated protein–protein interactions have been studied for a long time using theoretical, simulation and experimental approaches, but a full characterization of the thermodynamics and the dynamics on realistic systems is still lacking. In fact, it is typically difficult to measure experimentally the free energy of binding between two proteins in a lipid membrane. Early thermodynamic measurements were based on analytical ultracentrifuge experiments, which are difficult to interpret (MacKenzie and Fleming, 2008). Transmembrane helix interactions are often characterized using molecular-biology based assays (Fink et al., 2012), but these not provide direct thermodynamic data even if they appear to correlate strongly with thermodynamic data. Fluorescence assays appear to be one of the most powerful quantitative approaches at the moment (He and Hristova, 2012).

In the present work we calculated the free energy of association of model peptides in three different membrane systems, using a coarse-grained model with near-atomic resolution. We found no free energy barrier that fully dissociated helices must overcome to reach the associated state. This is in contrast with findings by Lague et al. (2001) who applied the hypernetted chain integral equation formalism, and by de Meyer et al. (2008) who used Dissipative Particle Dynamics (DPD) and a coarse-grained model with similar resolution as ours. We also found that, despite the absence of specific interaction, WALP23 peptides experience a significant attractive force in lipid membranes at all levels of hydrophobic mismatch. This result is qualitatively consistent with the above-mentioned theoretical and simulation studies, with our previous study (Monticelli et al., 2010) and with experimental studies on the same system (Sparr et al., 2005a) as well as with simulation studies on Glycophorin A (Henin et al., 2005; Janosi et al., 2010a,b; Orzaez et al., 2005; Sengupta and Marrink, 2010).

In our simulations, the association free energy for a WALP23 dimer is estimated to be greater than 20 kJ mol^{-1} in all bilayers, significantly larger compared to the predictions by Lague et al. (2001). Dimer stabilization free energy at contact calculated by de Meyer et al. (2008) is similar to ours in the case of positive hydrophobic mismatch and no mismatch, but is much lower in the case of negative mismatch. Experimental values for helix–helix dimerization vary over a significant range for different helices, but the closest system to our simulations is a leucine–alanine sequence $(AALALAA)_3$ in vesicles of varying lipid composition (Yano and Matsuzaki, 2006; Yano et al., 2006). Using a fluorescence assay, these authors measured a free energy of association $\Delta G_a = -12.7 \pm 0.4$ kJ mol^{-1}, an enthalpy change $\Delta H_a = -31.3 \pm 1.0$ kJ mol^{-1} and $-T\Delta S = 18.7 \pm 1.1$ kJ mol^{-1} for POPC lipids. These values compare to the calculated values in DOPC for WALP23 of $\Delta G_a = -20$ kJ mol^{-1}, an enthalpy change $\Delta H_a = -28$ kJ mol^{-1} and $-T\Delta S = 8$ kJ mol^{-1}. With the currently available data and the present set of MARTINI simulations it is difficult to assess the sources of the differences but the sign of the contributions and the approximate values are in agreement. Yano and Matsuzaki (2006) measured a range of −9 to −26 kJ mol^{-1} for association of $(AALALAA)_3$ in large unilamellar vesicles of monounsaturated lipids from C14 to C22 tails.

Helix association appears to be enthalpically favorable in all lipid bilayers, while the entropic contribution is favorable only in the case of positive hydrophobic mismatch (DMPC). Focusing on the enthalpic component, protein–protein and lipid–lipid interactions are the major forces driving helix association. This result supports the general conclusions drawn in theoretical dimerization studies of GpA helices in lipid membranes (Sengupta and Marrink, 2010).

Individual WALP23 peptides cause a certain perturbation in membrane properties such as mass density, membrane thickness and lipid ordering. The perturbation extends to 2–2.5 nm, consistent with predictions based on integral equations (Lague et al., 2001). As two peptides approach each other, the perturbed regions of the membrane fuse and their area decreases, leading to a favorable enthalpic contribution from lipid–lipid interactions.

Association of WALP23 peptides in the parallel and antiparallel orientation results in similar free energy profiles in DOPC and DPPC, but not in DMPC bilayers, where the helix-bilayer hydrophobic mismatch is greater. The anti-parallel orientation is preferred in DMPC mostly as a result of a more favorable entropic contribution, as well as protein–protein and lipid–lipid interaction energy.

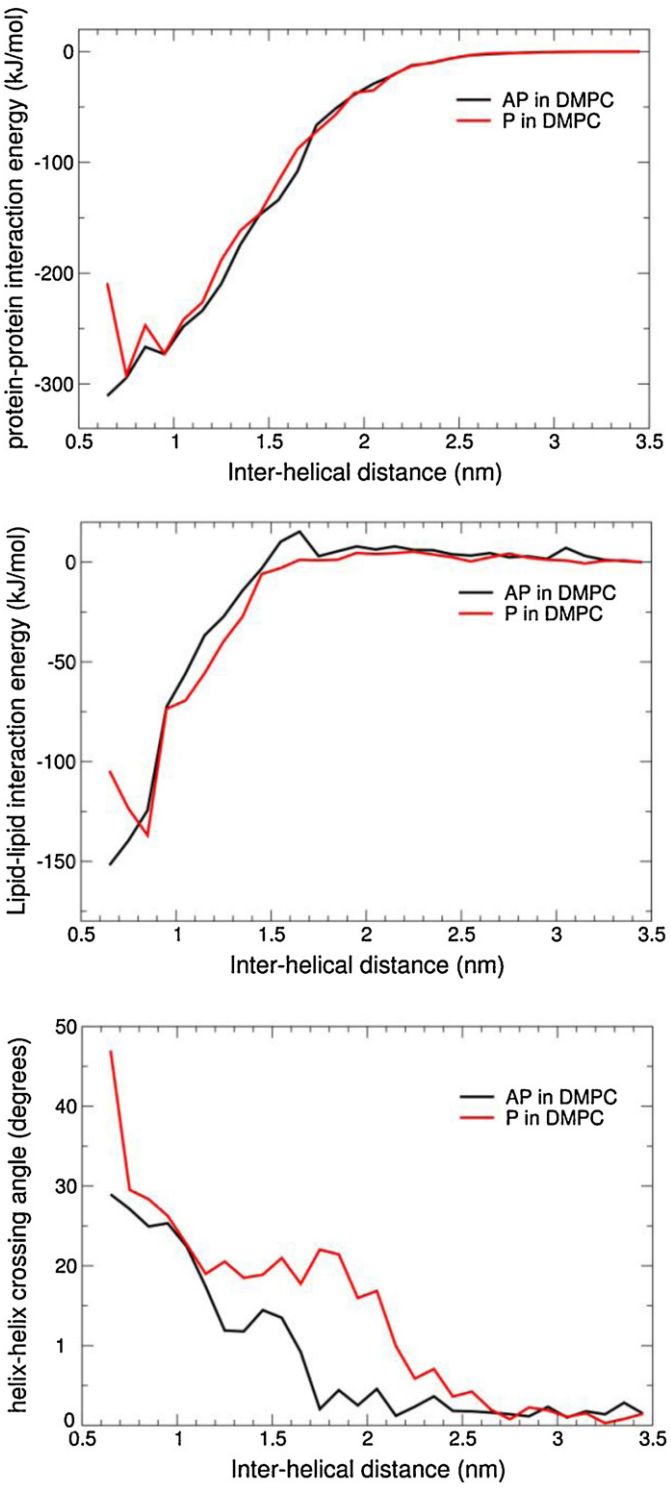

Fig. 9. Helix–helix interaction energy (top), lipid–lipid interaction energy (middle) and helix–helix crossing angle profiles of antiparallel (black) and parallel (red) association of WALP23 helices in DMPC. (For interpretation of the references to color in this figure legend, the reader is referred to the web version of this article.)

The more favorable protein–protein interaction energy is consistent with previous docking results, showing that the antiparallel orientation provides better surface complementarity (Monticelli et al., 2010) and that anti-parallel dimers are more stable particularly at high values of hydrophobic mismatch (Monticelli et al., 2010). However, in biological membrane proteins helix–helix interactions are determined by the membrane protein topology, such as in the case of dimerization of receptor tyrosine kinases with a single transmembrane span. For a detailed interpretation of the structure of possible WALP23 dimers experimental data is required.

Our results show that the potential energy barrier for helix association depends on the nature of the lipid membrane. Since no barrier was observed in the PMFs, a balanced entropic effect originated by the displacement of lipids along the process must be acting to compensate the potential energy cost of the association event. Such an entropic effect, which is related to the increase in the number of accessible states of the system, is particularly noteworthy in the case of DMPC. The profiles of the structural properties and lipid density plots suggest that the conformational space visited by the helices is larger in DMPC than in DPPC and DOPC. WALP23 helices exhibit greater tilt and crossing angle, and are more mobile in DMPC than in DPPC and DOPC. These differences in structural properties are clearly reflected by the density plots where the molecular ordering is significantly more disrupted in DMPC than DPPC and DOPC.

The simulations in this study show that it is possible to get detailed thermodynamic data that can be compared to experimental measurements, while at the same time giving access to properties that cannot be easily measured, including membrane deformation, lipid–helix interactions, and the structure and dynamics of the helices in a realistic bilayer environment. Although WALP23 is a model peptide, it is likely that a similar approach will work on biologically more important transmembrane helices, such as those in receptor tyrosine kinases or other signaling proteins. In addition, interactions between pairs of helices should add up to interactions in a full membrane protein, providing access by computer simulations to a thermodynamic model of membrane protein folding and stability in the not-too-distant future.

5. Conclusions

The associated state is significantly favored over the fully dissociated state for WALP23 helices embedded in lipid membranes, and there is no free energy barrier preventing the association of helices. Estimates of the association free energy in the systems simulated are greater than 20 kJ mol^{-1}, within the range of experimental values for a similar peptide Helix–helix and lipid–lipid interactions are the main driving forces for helix association. The association free energy profiles for both types of associations, antiparallel and parallel, exhibit deeper minima as the hydrophobic mismatch between the protein and the lipid bilayer increases (DMPC > DPPC > DOPC). Helix–helix interactions are found to be similar in the three bilayers, which is consistent with the similar packing of helices indicated by the crossing angle profiles. The difference between the dynamics of antiparallel and parallel association depends on the hydrophobic mismatch. The free energy profiles for both types of association are significantly different in DMPC. However, such difference is decreased in DPPC and basically not observed in DOPC. Helix–helix interactions are more favorable in the antiparallel association than those in the parallel association. We also introduced new analyses programs that will be useful for further detailed studies of helix–helix interactions.

Acknowledgements

This work was supported by the Canadian Institutes for Health Research, grant MOP-62690. NC was an Alberta Innovates Health Solutions (AIHS) Postdoctoral fellow. DPT is an AIHS Scientist and Alberta Innovates Technology Futures Strategic Chair in (Bio) Molecular Simulation. Simulations were carried out on WestGrid/Compute Canada facilities.

Appendix A. Supplementary data

Supplementary data associated with this article can be found, in the online version, at http://dx.doi.org/10.1016/j.chemphyslip.2013.02.001.

References

Ash, W.L., 2009. Helix–helix interactions in membrane proteins probed with computer simulations. Biological Sciences, University of Calgary, Calgary.

Benjamini, A., Smit, B., 2012. Robust driving forces for transmembrane helix packing. Biophysical Journal 103, 1227–1235.

Berendsen, H.J.C., Postma, J.P.M., van Gunsteren, W.F., Di Nola, A., Haak, J.R., 1984. Molecular dynamics with coupling to an external bath. Journal of Chemical Physics 81, 3684–3690.

Cymer, F., Veerappan, A., Schneider, D., 2012. Transmembrane helix–helix interactions are modulated by the sequence context and by lipid bilayer properties. Biochimica Et Biophysica Acta-Biomembranes 1818, 963–973.

de Meyer, F.J.M., Venturoli, M., Smit, B., 2008. Molecular simulations of lipid-mediated protein–protein interactions. Biophysical Journal 95, 1851–1865.

de Planque, M.R., Killian, J.A., 2003. Protein-lipid interactions studied with designed transmembrane peptides: role of hydrophobic matching and interfacial anchoring. Molecular Membrane Biology 20, 271–284.

de Planque, M.R.R., Goormaghtigh, E., Greathouse, D.V., Koeppe II, R.E., Kruijtzer, J.A.W., Liskamp, R.M.J., de Kruijff, B., Killian, J.A., 2001. Sensitivity of single membrane-spanning alpha-helical peptides to hydrophobic mismatch with a lipid bilayer: effects on backbone structure, orientation, and extent of membrane incorporation. Biochemistry 40, 5000–5010.

de Planque, M.R.R., Greathouse, D.V., Koeppe, R.E., Schafer, H., Marsh, D., Killian, J.A., 1998. Influence of lipid/peptide hydrophobic mismatch on the thickness of diacylphosphatidylcholine bilayers. A H-2 NMR and ESR study using designed transmembrane alpha-helical peptides and gramicidin A. Biochemistry 37, 9333–9345.

Doherty, G.J., McMahon, H.T., 2009. Mechanisms of endocytosis. Annual Review of Biochemistry 78, 857–902.

Driessen, A.J.M., Nouwen, N., 2008. Protein translocation across the bacterial cytoplasmic membrane. Annual Review of Biochemistry 77, 643–667.

Fink, A., Sal-Man, N., Gerber, D., Shai, Y., 2012. Transmembrane domains interactions within the membrane milieu: principles, advances and challenges. Biochimica Et Biophysica Acta-Biomembranes 1818, 974–983.

Fleming, K.G., Engelman, D.M., 2001. Specificity in transmembrane helix-helix interactions can define a hierarchy of stability for sequence variants. Proceedings of the National Academy of Sciences 98, 14340–14344.

Giacomini, K.M., Huang, S.M., Tweedie, D.J., Benet, L.Z., Brouwer, K.L.R., Chu, X.Y., Dahlin, A., Evers, R., Fischer, V., Hillgren, K.M., Hoffmaster, K.A., Ishikawa, T., Keppler, D., Kim, R.B., Lee, C.A., Niemi, M., Polli, J.W., Sugiyama, Y., Swaan, P.W., Ware, J.A., Wright, S.H., Yee, S.W., Zamek-Gliszczynski, M.J., Zhang, L., International, T., 2010. Membrane transporters in drug development. Nature Reviews Drug Discovery 9, 215–236.

He, L.J., Hristova, K., 2012. Physical–chemical principles underlying RTK activation, and their implications for human disease. Biochimica Et Biophysica Acta-Biomembranes 1818, 995–1005.

Henin, J., Pohorille, A., Chipot, C., 2005. Insights into the recognition and association of transmembrane alpha-helices. The free energy of alpha-helix dimerization in glycophorin A. Journal of the American Chemical Society 127, 8478–8484.

Hess, B., Kutzner, C., van der Spoel, D., Lindahl, E., 2008. GROMACS 4: algorithms for highly efficient, load-balanced, and scalable molecular simulation. Journal of Chemical Theory and Computation 4, 435–447.

Janosi, L., Prakash, A., Doxastakis, M., 2010a. Lipid-modulated sequence-specific association of glycophorin a in membranes. Biophysical Journal 99, 284–292.

Janosi, L., Prakash, A., Doxastakis, M., 2010b. Lipid-modulated sequence-specific association of glycophorin A in membranes. Biophysical Journal 99, 284–292.

Kandasamy, S.K., Larson, R.G., 2006. Molecular dynamics simulations of model transmembrane peptides in lipid bilayers: a systematic investigation of hydrophobic mismatch. Biophysical Journal 90, 2326–2343.

Kandt, C., Ash, W.L., Tieleman, D.P., 2007. Setting up and running molecular dynamics simulations of membrane proteins. Methods 41, 475–488.

Killian, J.A., Nyholm, T.K.M., 2006. Peptides in lipid bilayers: the power of simple models. Current Opinion in Structural Biology 16, 473–479.

Kim, T., Im, W., 2010. Revisiting hydrophobic mismatch with free energy simulation studies of transmembrane helix tilt and rotation. Biophysical Journal 99, 175–183.

Kumar, S., Bouzida, D., Swendsen, R.H., Kollman, P.A., Rosenberg, J.M., 1992. The weighted histogram analysis method for free-energy calculations on biomolecules.1. The method. Journal of Computational Chemistry 13, 1011–1021.

Lague, P., Zuckermann, M.J., Roux, B., 2001. Lipid-mediated interactions between intrinsic membrane proteins: dependence on protein size and lipid composition. Biophysical Journal 81, 276–284.

Langosch, D., Arkin, I.T., 2009. Interaction and conformational dynamics of membrane-spanning protein helices. Protein Science 18, 1343–1358.

Li, E., Wimley, W.C., Hristova, K., 2012. Transmembrane helix dimerization: beyond the search for sequence motifs. Biochimica Et Biophysica Acta-Biomembranes 1818, 183–193.

MacCallum, J.L., Moghaddam, M.S., Chan, H.S., Tieleman, D.P., 2007. Hydrophobic association of alpha-helices, steric dewetting, and enthalpic barriers to protein folding. Proceedings of the National Academy of Sciences 104, 6206–6210.

MacCallum, J.L., Tieleman, D.P., 2011. Hydrophobicity scales: a thermodynamic looking glass into lipid–protein interactions. Trends in Biochemical Sciences 36, 653–662.

MacKenzie, K.R., Fleming, K.G., 2008. Current Opinion in Structural Biology 18, 412–419.

Marrink, S.J., Risselada, H., Yefimov, j.S., Tieleman, D.P., de Vries, A.H., 2007. The MARTINI force field: coarse grained model for biomolecular simulations. The Journal of Physical Chemistry B 11, 7812–7824.

Monticelli, L., Kandasamy, S.K., Periole, X., Larson, R.G., Tieleman, D.P., Marrink, S.J., 2008. The MARTINI coarse-grained force field: extension to proteins. Journal of Chemical Theory and Computation 4, 819–834.

Monticelli, L., Tieleman, D.P., Fuchs, P.F.J., 2010. Interpretation of H-2-NMR experiments on the orientation of the transmembrane helix WALP23 by computer simulations. Biophysical Journal 99, 1455–1464.

Orzaez, M., Lukovic, D., Abad, C., Perez-Paya, E., Mingarro, I., 2005. Influence of hydrophobic matching on association of model transmembrane fragments containing a minimised glycophorin A dimerisation motif. FEBS Letters 579, 1633–1638.

Periole, X., Knepp, A.M., Sakmar, T.P., Marrink, S.J., Huber, T., 2012. Structural determinants of the supramolecular organization of G protein-coupled receptors in bilayers. Journal of the American Chemical Society 134, 10959–10965.

Psachoulia, E., Marshall, D.P., Sansom, M.S.P., 2010. Molecular dynamics simulations of the dimerization of transmembrane alpha-helices. Accounts of Chemical Research 43, 388–396.

Rosenbaum, D.M., Rasmussen, S.G.F., Kobilka, B.K., 2009. The structure and function of G-protein-coupled receptors. Nature 459, 356–363.

Roux, B., 1995. The calculation of the potential of mean force using computer-simulations. Computer Physics Communications 91, 275–282.

Schafer, L.V., de Jong, D.H., Holt, A., Rzepiela, A.J., de Vries, A., Poolman, B., Killian, J.A., Marrink, S.J., 2011. Lipid packing drives the segregation of transmembrane helices into disordered lipid domains in model membranes. Proceedings of the National Academy of Sciences 108, 1343–1348.

Sengupta, D., Marrink, S.J., 2010. Lipid-mediated interactions tune the association of glycophorin A helix and its disruptive mutants in membranes. Physical Chemistry Chemical Physics 12, 12987–12996.

Sparr, E., Ash, W.L., Nazarov, P.V., Rijkers, D.T.S., Hemminga, M.A., Tieleman, D.P., Killian, J.A., 2005a. Self-association of transmembrane alpha-helices in model membranes - Importance of helix orientation and role of hydrophobic mismatch. The Journal of Biological Chemistry 280, 39324–39331.

Sparr, E., Ganchev, D.N., Snel, M.M.E., Ridder, A.N.J.A., Kroon-Batenburg, L.M.J., Chupin, V., Rijkers, D.T.S., Killian, J.A., Kruijff, B.d., 2005b. Molecular organization in striated domains induced by transmembrane alpha-helical peptides in dipalmitoyl phosphatidylcholine bilayers. Biochemistry 44, 2–10.

Strandberg, E., Esteban-Martin, S., Ulrich, A.S., Salgado, J., 2012. Hydrophobic mismatch of mobile transmembrane helices: merging theory and experiments. Biochimica Et Biophysica Acta-Biomembranes 1818, 1242–1249.

Sudhof, T.C., Rothman, J.E., 2009. Membrane fusion: grappling with SNARE and SM proteins. Science 323, 474–477.

Torrie, G.M., Valleau, J.P., 1977. Non-physical sampling distributions in monte-carlo free-energy estimation - umbrella sampling. Journal of Chemical Physics 23, 187–199.

Vostrikov, V.V., Hall, B.A., Greathouse, D.V., Koeppe II, R.E., Sansom, M.S.P., 2010. Changes in transmembrane helix alignment by arginine residues revealed by solid-state NMR experiments and coarse-grained MD simulations. Journal of the American Chemical Society 132, 5803–5811.

White, S.H., von Heijne, G., 2004. Transmembrane helices before, during, and after insertion. Current Opinion in Structural Biology 14, 397–404.

Wimley, W.C., 2012. Protein folding in membranes. Biochimica Et Biophysica Acta-Biomembranes 1818, 925–926.

Woolhead, C.A., McCormick, P.J., Johnson, A.E., 2004. Nascent membrane and secretory proteins differ in FRET-detected folding far inside the ribosome and in their exposure to ribosomal proteins. Cell 116, 725–736.

Wu, Z., Cui, Q., Yethiraj, A., 2011. Driving force for the association of hydrophobic peptides: the importance of electrostatic interactions in coarse-grained water models. Journal of Physical Chemistry Letters 2, 1794–1798.

Yano, Y., Matsuzaki, K., 2006. Measurement of thermodynamic parameters for hydrophobic mismatch 1: self-association of a transmembrane helix. Biochemistry 45, 3370–3378.

Yano, Y., Ogura, M., Matsuzaki, K., 2006. Measurement of thermodynamic parameters for hydrophobic mismatch 2: intermembrane transfer of a transmembrane helix. Biochemistry 45, 3379–3385.

Yano, Y., Takemoto, t., Kobayashi, S., Yasui, H., Sakurai, H., Ohashi, W., Niwa, M., Futaki, S., Sugiura, Y., Matsuzaki, K., 2002. Topological stability and self-association of a completely hydrophobic model transmembrane helix in lipid bilayers. Biochemistry 41, 3073–3080.

Yano, Y., Yamamoto, A., Ogura, M., Matsuzaki, K., 2011. Thermodynamics of insertion and self-association of a transmembrane helix: a lipophobic interaction by phosphatidylethanolamine. Biochemistry 50, 6806–6814.